

Collisions of Dark Solitons in Elongated Bose-Einstein Condensates

S. Stellmer,¹ C. Becker,¹ P. Soltan-Panahi,¹ E.-M. Richter,¹ S. Dörscher,¹ M. Baumert,¹
J. Kronjäger,¹ K. Bongs,² and K. Sengstock^{1,*}

¹*Institut für Laser-Physik, Universität Hamburg, Luruper Chaussee 149, 22761 Hamburg, Germany*

²*MUARC, School of Physics and Astronomy, University of Birmingham, Edgbaston, Birmingham B15 2TT, United Kingdom*
(Received 13 May 2008; published 19 September 2008)

We present experimental data showing the head-on collision of dark solitons generated in an elongated Bose-Einstein condensate. No discernable interaction can be recorded, in full agreement with the fundamental theoretical concepts of solitons as mutually transparent quasiparticles. Our soliton generation technique allows for the creation of solitons with different depths; hence, they can be distinguished and their trajectories be followed. Simulations of the 1D-Gross-Pitaevskii equation have been performed to compare the experiment with a mean-field description.

DOI: [10.1103/PhysRevLett.101.120406](https://doi.org/10.1103/PhysRevLett.101.120406)

PACS numbers: 03.75.Lm, 05.45.Yv, 42.65.Tg, 67.85.De

Nonlinear systems give rise to a wealth of phenomena, among which solitons emerged to play a prominent role. Solitons appear as wave packets that preserve their amplitude and shape during propagation and even persist unchanged from collisions with one another, therefore being attributed a particlelike character. Solitons in nonlinear media were described numerically [1] and analytically [2] some 40 years ago and have been identified in fields as diverse as oceanography, neural networks and fiber optics. So-called *dark* solitons emerge as localized dips of the background medium, presenting a unique balance between the defocusing dispersion and a focusing repulsive nonlinear interaction.

Bose-Einstein condensates (BEC) in dilute atomic vapors represent a completely new and largely tunable system, in which many nonlinear phenomena such as four-wave mixing [3], vortices [4–6], and bright solitons [7–10] have been explored, to name only a few examples. As yet another paradigm, dark solitons have been created by phase imprinting [11–13], density engineering [14], sweeping a dipole potential through the condensate [15], as a consequence of quantum shock [16,17], and from the local minima of interference fringes [18,19]. The stability of these excitations has been investigated both theoretically (see, e.g. [20,21]) and experimentally, as well as their dependence on dimensionality [22]. As a manifestation of the particlelike character, oscillations in a conservative external potential have been predicted [23,24] and very recently been observed [13,19]. The interaction between solitons has been of fundamental interest from the very beginning [25–28], and has lately been studied in the context of the new experimental realizations [29,30].

In general, the collisions of solitons are a very active area of research and different regimes have been studied so far. The presence of two solitonlike structures within a finite nonlinear system is highly nontrivial, since a superposition of two solutions is not necessarily a solution as well. It was shown [2] that two solitons asymptotically

retain their shapes for large separations. The “chase” scenario (two solitons with different velocities traveling in the same direction such that one eventually overtakes the other one) can be described by the inverse scattering transform [25]. Because of the interaction, only a very small shift in their trajectories as compared to the unperturbed case will occur [26] and can be calculated analytically: the solitons pass through one another and regain their initial configuration. This can also be shown by taking the viewpoint of momentum conservation [28]. The case of a “head-on” collision, however, cannot be described by the inverse scattering transform [29]. Numerical simulations [27,31] and analytic calculations [25,29,30] have shown a positive shift after the collision.

A recent experiment [19] investigated the interaction of dark solitons in an harmonic potential and observed a substantial deviation of the oscillation frequency from the characteristic value of the axial trapping frequency ω_z divided by $\sqrt{2}$. The upshift could be explained by corrections due to the imperfect 1D geometry as well as the interaction between the solitons.

In this Letter, we explore the actual collisional dynamics in a quite different regime. We employ a phase-imprinting method that enables us to set the positions and depths of the two dark solitons independently, thus making them distinguishable. Furthermore, we choose an axial confinement which is weaker by an order of magnitude, leading to a tenfold larger oscillation period. This way, we can track each soliton for hundreds of milliseconds.

Before we commence, let us briefly turn to nonlinear optics, a well-explored field that comprises optical dark solitons as a direct analogue to dark solitons in quantum gases [32]. Here, the field-dependent index of refraction of nonlinear optical media allows for different types of solitons. While both spatial and temporal *bright* optical solitons (well-localized rays of light and stable pulses, respectively) are the more obvious species and have developed into a telecommunication standard, optical *dark* sol-

itons enjoy a distinguished interest of their own [33]. For temporal dark solitons (intensity dips in a pulse of light), repulsive interaction has been observed [34], the same holds for spatial dark solitons [35]. It is only in nonlocal nonlinear media that the interaction can even be tuned to attraction [36].

Let us now turn to the description of dark solitons in BEC. In the mean-field regime, the dynamics of a BEC can be described by the well-known Gross-Pitaevskii equation (GPE), whose one-dimensional form reads

$$i\hbar\dot{\Psi}(z, t) = -\frac{\hbar^2}{2m}\Psi''(z, t) + [V_{\text{ext}}(z) + g|\Psi(z, t)|^2]\Psi(z, t) \quad (1)$$

and supports solutions of the form

$$\Psi_D(z, t) = \sqrt{n_0} \left[i \frac{\dot{q}}{c_s} + \sqrt{1 - \frac{\dot{q}^2}{c_s^2}} \tanh[\kappa(z - q(t))] \right] e^{(gn_0 t / i\hbar)}. \quad (2)$$

These are identified as dark solitons. Here, Ψ denotes the wave function of the condensate, V_{ext} the external potential, and $g = 2\hbar\omega_{\perp}a$ measures the interatomic interaction where a is the s -wave scattering length, ω_{\perp} the transverse trapping frequency, and m the atomic mass. Furthermore, n_0 denotes the maximum density of the condensate, q the position of the soliton plane, and $c_s = \sqrt{ng/2m}$ the local speed of sound. The size of the soliton is determined by the parameter $\kappa = \xi^{-1}\sqrt{1 - (\dot{q}/c_s)^2}$, it is on the order of the healing length $\xi = \hbar/mc_s$. Note that this formalism applies only to the homogeneous one-dimensional case.

The connection between the depth n_s of the density dip, its velocity \dot{q} and the associated phase jump ϕ across the nodal plane is given by

$$\frac{n_s}{n_0} = 1 - \left(\frac{\dot{q}}{c_s}\right)^2 = \sin^2\left(\frac{\phi}{2}\right). \quad (3)$$

Only a completely “black” soliton in the minimum of the trapping potential corresponds to a time-independent solution of Eq. (1). For any other configuration, the phase gradient will induce a superfluid flow across the soliton plane, causing it to propagate within the BEC under the influence of the trapping potential. It is the phase jump that we employ to create solitons: A phase gradient between 0 and π with an extension on the order of the healing length ξ will evolve into a dark soliton [11]. The local phase evolution, in turn, is suitably tailored by an optical dipole potential.

Experimental technique.—The experimental procedure is as follows: 5×10^9 atoms of ^{87}Rb are trapped in a magneto-optical trap and afterwards compressed and cooled in an optical molasses. Subsequent evaporative cooling in a magnetic trap takes place before the atoms are loaded into an optical dipole trap. After further evaporative cooling over 20 s, a quasi one-dimensional and al-

most pure BEC of about 5×10^4 atoms in the $|5^2S_{1/2}, F = 1, m_F = -1\rangle$ state is produced with a chemical potential of less than 20 nK. The trap frequencies read $\omega_{z,\text{ver},\text{hor}} = 2\pi \times (5.9, 85, 133)$ Hz. The peak density of $n_0 = 5.8 \times 10^{13} \text{ cm}^{-3}$ translates into a speed of sound $c_s = 1.0 \text{ mm/s}$ and a healing length of $\xi = 0.7 \mu\text{m}$.

A laser pulse of 70 μs duration, detuned from resonance by 8 GHz to the blue, is used for the phase imprinting. For local access, we employ a spatial light modulator to design the intensity profile of the light with a resolution of better than 2 μm at the position of the condensate. In this way, the number of solitons created can be varied, as can their individual depths, initial positions and directions of movement be chosen over a wide range of parameters by tailoring the nearly arbitrarily shapeable light field potentials acting on the BEC. For the experiment described here, we image a two-step intensity profile onto the BEC, thus creating one soliton at each phase step (Fig. 1).

We generate two solitons with slightly different depths in such a way that they propagate to opposite sides of the condensate, are reflected there, approach one another and eventually collide in the center of the trap. This approach is

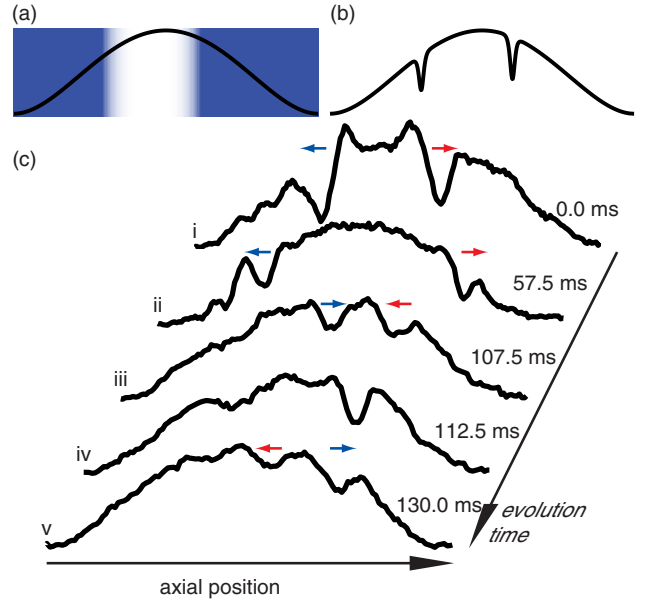


FIG. 1 (color online). (a),(b) Scheme of the phase-imprinting method. A rectangular intensity profile as shown is imaged onto the condensate (a) to generate one soliton at each intensity step of the far-detuned light field. The sign of the detuning is chosen such that the solitons propagate to the edges of the condensate. Following Eq. (3), the depths n_s of the emerging solitons (b) depend on the local background density n_0 and are different for the asymmetric configuration. (c) Evolution of the solitons in the trap. Absorption images of the BEC are integrated in the transverse directions to obtain the density distribution along the axial coordinate. The pictures show experimental snapshots of solitons shortly after creation (i), at the edges of the condensate (ii), and shortly before (iii), at (iv), and after collision (v).

chosen for various reasons. (i) The observed oscillation frequency when first propagating “independently” is used to identify the density modulation as dark solitons with characteristic oscillation frequencies $\Omega = \omega_z/\sqrt{2}$. (ii) As the residual density of the solitons can only be determined with a large uncertainty, we use the amplitude of their oscillation, which directly depends on the depth n_s , to tag the individual solitons. The oscillation amplitudes can be measured prior to the first collision. (iii) Any *rapid* decay mechanism of the solitons via noncontact, long-range interaction (e.g. phonon scattering), should it exist, would be observed as a dampening prior to the first collision. (iv) Density waves and other excitations originating from the imperfect imprinting method will be dampened during the precollision time, leaving two well-characterized dark solitons on an almost uniform background.

Experimental results.—After a variable evolution time of the soliton dynamics in the BEC, we switch off the trapping potential and allow for a free expansion of 11 ms. Afterwards, we take an absorption image of the condensate. A time series of the axial optical density of the BEC is shown in Fig. 2(a). As can be clearly inferred, the two initial solitons propagate to the edges of the condensate, are reflected there and then propagate through one another. Clearly they neither annihilate, nor split up into a number of smaller solitons, nor form a bound state. Two density waves carrying away the excess density can be observed as well during the first 25 ms. The corresponding space-time plot of the density minima [Fig. 2(b)] is used to determine the oscillation frequencies to be $\Omega_1 = 2\pi \times 3.5$ Hz and $\Omega_2 = 2\pi \times 3.8$ Hz. The deviation from the theoretical value $\Omega = \omega_z/\sqrt{2}$ can be explained by the anharmonicity of the trap [13]. The relative oscillation amplitudes of $Z_1 = 0.55$ and $Z_2 = 0.60$ correspond to relative depths n_s/n_0 of the dip of 0.74 and 0.69 in the incident of collision for soliton 1 and 2, respectively. The scatter is due to shot-to-shot fluctuations, e.g., of the atom number and power of the phase-imprinting laser. Furthermore, acceleration due to thermal collisions is also temperature dependent [21,37,38] and may fluctuate as well. The scatter increases with evolution time and, together with a decrease in contrast, renders a precise and reproducible determination of the soliton position impossible for evolution times beyond 200 ms. By comparison of the oscillation amplitudes before and after the collision, we can show that the solitons indeed pass through one another and retain their characteristics. We employed a fit to the data assuming a “reflection” during collision, but find a much weaker agreement. This clearly favors a behavior of “passing” through each other instead of being reflected as sometimes discussed in the context of soliton physics. Of course, the individual identity of solitons as quasiparticles breaks down if close to one another, particularly since momentum transfer can occur during

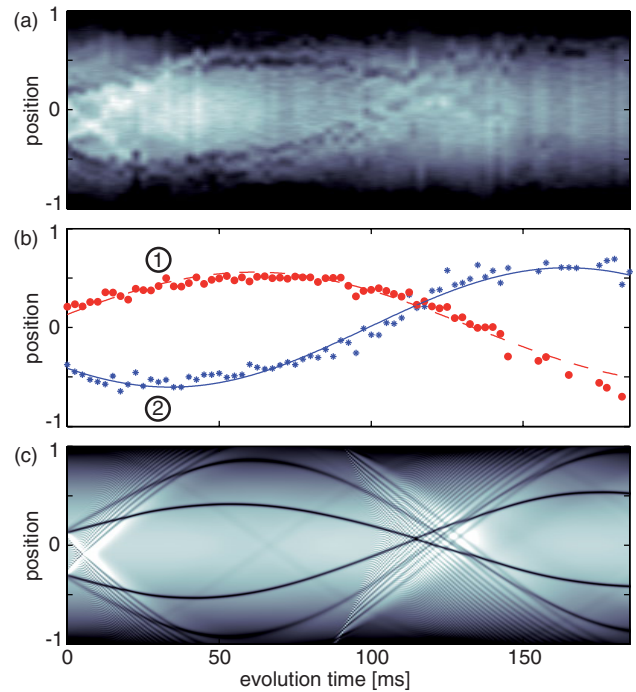


FIG. 2 (color online). Space-time plots of two solitons oscillating in a confining potential. Positions are normalized to the condensate extension to correct for quadrupole oscillations, which exhibit a relative amplitude of around 0.14 but do not couple to the soliton movement [23], and to reduce influences from fluctuations of the atom number. (a) Experimental observation. Time steps of evolution of the BEC in the trap are 2.5 ms. (b) A sinusoidal fit to the soliton positions at each time step. Note that the choice of asymmetric starting points of the two solitons results in different depths and therefore allows for the “identification” of the solitons as 1 (colored red, deeper, smaller oscillation amplitude) and 2 (colored blue, shallower, larger oscillation amplitude); see the text for details. The error bars in both time and position are well within the marks. (c) Numerical simulation of the 1D-GPE set to our parameters. Additional smaller solitons, only faintly visible in (a), can also be observed [13].

collision [29]. From this perspective, the color coding of Fig. 2(b) is too simplistic, but it emphasizes the fact that for long times after the collision, the observed states correspond to two solitons propagating as if they were unperturbed by one another. Furthermore, our measurements set an upper limit for a significant damping mechanism due to long-range soliton interaction mediated by the incoherent scattering of phonons [39]: since the lifetime is about the same as with only one soliton present [13], a decay rate larger than ω_z can be excluded.

Numerical simulations.—We perform numerical simulations of the 1D-GPE to compare the experimental data with a mean-field description [Fig. 2(c)]. The simulations take into account the independently determined experimental parameters (trapping potential and particle number) and fully incorporate the phase-imprinting method through

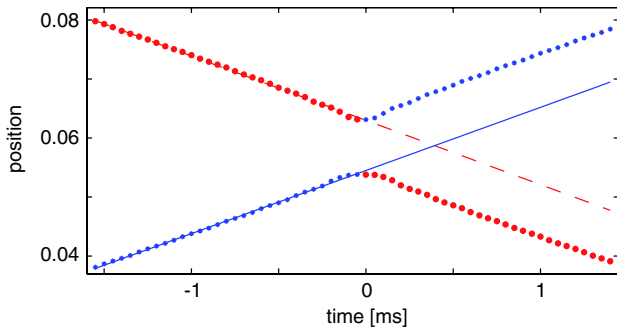


FIG. 3 (color online). A close-up simulation of the collision with a resolution of 0.05 ms, given in the representation of Fig. 2 (b). Lines indicate trajectories without interaction.

a time evolution, thus showing all the generic features of the experiment except for finite temperature effects, like damping. An excellent agreement can be seen.

A possible position shift due to the interaction has been investigated in many theoretical works and with different methods. Given our experimental parameters, a positive shift of $\Delta x \approx 0.015 \mu\text{m}$ (with respect to the unperturbed trajectory of a single soliton) is predicted analytically [29]. A shift of $\Delta x = 0.51 \mu\text{m}$ can be retrieved from a different analytic model [25,30]. These shifts are smaller than the optical resolution of a typical BEC-experiment of a few μm , and cannot be resolved in our regime.

The simulation, however, can indeed be used to investigate the details of the collision: a close-up of the collision is given in Fig. 3. The trajectories exhibit positive shifts of $\Delta x_r = 0.4 \mu\text{m}$ and $\Delta x_b = 0.5 \mu\text{m}$, corresponding to roughly 0.01 in the normalized units of Fig. 2. Given our values of n_s , we expect only one depression of zero density during the process of collision [40].

In conclusion, we have presented a direct observation of two colliding dark solitons in a BEC, thereby verifying the concept of nondestructive transmission. Numerical simulations agree very well with the experiment and have been used to study the shift in trajectories. Future experiments may seek to detect a significant change in position, possibly in a different geometry (increased trap frequency or ring traps), or by a significantly smaller velocity difference to allow for longer interaction times. By variation of the initial soliton depths, it might be possible to search for a velocity dependence of the interaction.

We thank the Deutsche Forschungsgemeinschaft DFG for funding within the Forschergruppe FOR801 and the GRK 1355. K.B. thanks EPSRC for financial support in grant EP/E036473/1.

*sengstock@physnet.uni-hamburg.de

- [1] N.J. Zabusky, Phys. Rev. **168**, 124 (1968).
- [2] V.E. Zakharov and A.B. Shabat, Sov. Phys. JETP **34**, 62 (1972).
- [3] L. Deng *et al.*, Nature (London) **398**, 218 (1999).
- [4] M.R. Matthews *et al.*, Phys. Rev. Lett. **83**, 2498 (1999).
- [5] K.W. Madison *et al.*, Phys. Rev. Lett. **84**, 806 (2000).
- [6] A.E. Leanhardt *et al.*, Phys. Rev. Lett. **90**, 140403 (2003).
- [7] K.E. Strecker *et al.*, Nature (London) **417**, 150 (2002).
- [8] L. Khaykovich *et al.*, Science **296**, 1290 (2002).
- [9] S.L. Cornish *et al.*, Phys. Rev. Lett. **96**, 170401 (2006).
- [10] B. Eiermann *et al.*, Phys. Rev. Lett. **92**, 230401 (2004).
- [11] S. Burger *et al.*, Phys. Rev. Lett. **83**, 5198 (1999).
- [12] J. Denschlag *et al.*, Science **287**, 97 (2000).
- [13] C. Becker *et al.*, Nature Phys. **4**, 496 (2008).
- [14] B.P. Anderson *et al.*, Phys. Rev. Lett. **86**, 2926 (2001).
- [15] P. Engels and C. Atherton, Phys. Rev. Lett. **99**, 160405 (2007).
- [16] Z. Dutton *et al.*, Science **293**, 663 (2001).
- [17] J.J. Chang *et al.*, arXiv:0803.2535 [Phys. Rev. Lett. (to be published)].
- [18] G.B. Jo *et al.*, Phys. Rev. Lett. **98**, 180401 (2007).
- [19] A. Weller *et al.*, arXiv:0803.4352 [Phys. Rev. Lett. (to be published)].
- [20] A.E. Muryshev *et al.*, Phys. Rev. A **60**, R2665 (1999).
- [21] P.O. Fedichev *et al.*, Phys. Rev. A **60**, 3220 (1999).
- [22] G. Theocharis *et al.*, Phys. Rev. A **76**, 045601 (2007).
- [23] T. Busch and J.R. Anglin, Phys. Rev. Lett. **84**, 2298 (2000).
- [24] V.V. Konotop and L. Pitaevskii, Phys. Rev. Lett. **93**, 240403 (2004).
- [25] V.E. Zakharov and A.B. Shabat, Sov. Phys. JETP **37**, 823 (1973).
- [26] T. Tszuzuki, J. Low Temp. Phys. **4**, 441 (1971).
- [27] N.J. Zabusky and M.D. Kruskal, Phys. Rev. Lett. **15**, 240 (1965).
- [28] P.D. Lax, Commun. Pure Appl. Math. **21**, 467 (1968).
- [29] G. Huang *et al.*, Phys. Rev. A **64**, 013617 (2001).
- [30] S. Burger *et al.*, Phys. Rev. A **65**, 043611 (2002).
- [31] L.D. Carr *et al.*, J. Phys. B **33**, 3983 (2000).
- [32] N.P. Proukakis *et al.*, J. Opt. B **6**, S380 (2004).
- [33] Y.S. Kivshar and B. Luther-Davies, Phys. Rep. **298**, 81 (1998).
- [34] D. Foursa and P. Emplit, Phys. Rev. Lett. **77**, 4011 (1996).
- [35] Y.S. Kivshar and W. Krolikowski, Opt. Commun. **114**, 353 (1995).
- [36] A. Dreischuh *et al.*, Phys. Rev. Lett. **96**, 043901 (2006).
- [37] B. Jackson *et al.*, Phys. Rev. A **75**, 051601 (2007).
- [38] A. Muryshev *et al.*, Phys. Rev. Lett. **89**, 110401 (2002).
- [39] N.G. Parker *et al.*, Phys. Rev. Lett. **90**, 220401 (2003).
- [40] Note that other regimes of zero or two touchdowns might exist for different combinations of n_s .